

Pinned Low-Energy Electronic Excitation in Metal-Exchanged Vanadium Oxide Nanoscrolls

J. Cao,[†] J. L. Musfeldt,^{*,†} S. Mazumdar,[‡] N. A. Chernova,[§] and M. S. Whittingham[§]

Department of Chemistry, University of Tennessee, Knoxville, Tennessee 37996-1600,

Department of Physics, University of Arizona, Tucson, Arizona 85721, and

*Department of Chemistry and Institute for Materials Research,
State University of New York, Binghamton, New York 13902-6000*

Received April 27, 2007; Revised Manuscript Received June 11, 2007

ABSTRACT

We measured the optical properties of mixed valent vanadium oxide nanoscrolls and their metal-exchanged derivatives in order to investigate the charge dynamics in these compounds. In contrast to the prediction of a metallic state for the metal-exchanged derivatives within a rigid band model, we find that the injected charges in Mn²⁺-exchanged vanadium oxide nanoscrolls are pinned. A low-energy electronic excitation associated with the pinned carriers appears in the far infrared and persists at low temperature, suggesting that the nanoscrolls are weak metals in their bulk form, dominated by inhomogeneous charge disproportionation and Madelung energy effects.

The discovery that low-dimensional inorganic solids can curve or fold into nanoscale objects provides an exciting opportunity to investigate bulk versus nanoscale chemistry using molecular-level strain as the tuning parameter.^{1–3} These materials are targets of intensive research efforts, driven by the need to further miniaturize electronic devices and the potential to exploit unusual mechanical and optical properties. Some of the beautiful, flexible, and functional nanomorphologies include tubes, wires, octahedra, particles, urchins, and spheres.^{1–9} They offer molecular-level control of size, shape, mechanical response, and chemical composition as well as unusual confinement effects due to finite length scales.

Among the transition-metal oxides, vanadates show particularly rich chemistry because of the tunable vanadium oxidation state and flexible coordination environment, which ranges from octahedral to square pyramidal to tetrahedral with increasing vanadium oxidation state.¹⁰ Vanadium oxides form many layered and nanoscale compounds with open structural frameworks, making them prospective materials for ion intercalation, exchange, and storage.^{7–9,11} The nanoscale vanadates of interest here, (amine)_yVO_x, are formally mixed-valent⁶ with $x \sim 2.4$ and $y \sim 0.28$. Stoichiometric considerations do not, of course, distinguish between a true mixed-valent V^{4.5+} state that may be metallic and a state with an inhomogeneous charge distribution, consisting of V

ions with distinct small and large charges. Such charge disproportionation is common in oxides of Ti and V with formal oxidation states of Ti^{3.5+} and V^{4.5+}, respectively, and the convention is to assign integer charges (Ti³⁺ and Ti⁴⁺; V⁴⁺ and V⁵⁺) to the ions with different oxidation states.^{12–14} We adopt the same convention here and consider the possibility of charge disproportionation in the nanoscale vanadates.

The compounds we consider are actually scrolls, consisting of vanadate sheets between which organic molecules are intercalated.^{6–8,15,16} The size of the amine or diamine template determines scroll winding, providing an opportunity to tune the size of these materials. The typical scrolls are ~ 15 – 100 nm in diameter, containing up to 30 vanadium oxide layers (inset of Figure 1a). The exact crystal structure is complicated and is not completely understood. Figure 1a shows a representative X-ray powder diffraction pattern for the (C₁₂H₂₅NH₃)_y–VO_x scrolls. The (00l) reflections from the vanadium oxide layers are clear, but the (hk0) reflections from the atomic structure within each layer are weak. The data suggest a tetragonal lattice of basal repeat size 6.144 Å, closely related to that of BaV₇O₁₆, which has a planar structure of basal size 6.160 Å.¹⁷ The arrangement in BaV₇O₁₆ is shown in Figure 1b.¹⁷ It contains zigzag chains of highly distorted edge-sharing VO₆ octahedra. The distortion is so strong (because of the large displacement of one apical oxygen) that the octahedra are often considered to be VO₅ square pyramids. These chains share some corners with each other to form a two-dimensional layer. The layers also

* Corresponding author. E-mail: musfeldt@utk.edu.

[†] University of Tennessee.

[‡] University of Arizona.

[§] State University of New York, Binghamton.

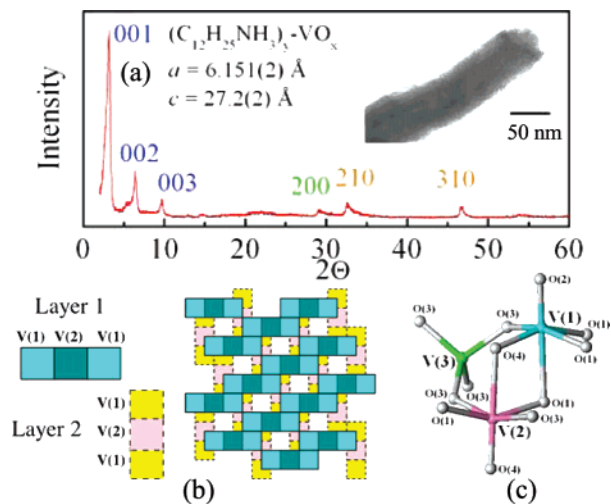


Figure 1. (a) Representative X-ray powder diffraction scan of $(\text{C}_{12}\text{H}_{25}\text{NH}_3)_y\text{-VO}_x$ scrolls showing only 00l and weak hk0 reflections. The inset displays a representative TEM image with lattice fringing and a center cavity. The interlayer spacing for the pristine scrolls is $27.2(2) \text{ \AA}$. (b) Probable double-layer structure of the VO_x scrolls, analogous to the $\text{BaV}_7\text{O}_{16}$ model compound.¹⁷ (c) Close-up view of the local structure around the V centers, showing the arrangement of octahedra and tetrahedra in the $\text{BaV}_7\text{O}_{16}$ model compound.¹⁷

share corners with VO_4 tetrahedra, bringing the two VO_x layers together to form a characteristic double sheet. Figure 1c displays the local structure around the V centers in the $\text{BaV}_7\text{O}_{16}$ model compound. Each two-dimensional sheet contains two octahedrally coordinated vanadium atoms, V(1) and V(2), with one tetrahedrally coordinated V(3) in between the layers.

Scrolled vanadates exhibit very interesting physical properties including a large spin gap, diameter-dependent optical features, and potential battery and optical limiting applications.^{18–23} Recently, electron- and hole-doped vanadium oxide nanoscrolls were reported to be 300 K ferromagnets, raising fundamental questions about introducing free carriers into the pristine Mott insulating scrolls, resulting in partially filled bands. The “doped” nanoscrolls are predicted to exhibit Drude-type metallic behavior within this picture.¹⁹ Direct measurement of the low-energy electronic structure is clearly important to test this prediction. Furthermore, the rigid band model raises fundamental questions about the chemical nature of the “doping” or ion-exchange process in the scrolled vanadates.^{16,19,24,25} From a chemical perspective, metal intercalation does not appear as simple as “putting in electrons”; both reduction of vanadium and ion exchange with the proton on the amine are possible consequences of the exchange process. To date, only Mn^{2+} has been shown to completely replace the organic template, even though some other ions such as Na^+ , Li^+ , Zn^{2+} , Cu^{2+} , and Ca^{2+} can partially replace the amine template.^{16,24,25} Metal exchange also reduces the interlayer spacing. For our materials, it decreases from $27.2(2) \text{ \AA}$ in the pristine scrolls to $10.5(3) \text{ \AA}$ upon Mn^{2+} substitution.²¹ Interestingly, the latter distance is comparable to what is observed in certain intercalated graphite systems.²⁶ For instance, the sheet-to-sheet distance in the CoCl_2 substituted system is 9.3 \AA .²⁶ Charge transfer

in intercalated graphite materials with sizable interlayer distances indicates similar charge injection in the exchanged vanadium oxide scrolls.

In order to understand the fundamental charge dynamics and test the applicability of the rigid band model in vanadium oxide nanoscrolls, we investigated the variable temperature optical spectra of the pristine and Mn^{2+} -exchanged materials. In contrast to the rigid band model expectation for a metallic state, we find that charge is pinned in the metal substituted scrolls. The low-energy electronic excitation associated with the pinned carriers appears in the far infrared and persists at low temperature, suggesting that the nanoscrolls are weak metals in their bulk form, dominated by inhomogeneous charge disproportionation and Madelung energy effects. We propose an alternate model for charge injection to account for our observations. Analysis of the vibrational properties shows that the 575 cm^{-1} V–O–V equatorial stretching mode is very sensitive to metal substitution, indicating that ion exchange modifies both the local curvature and the charge environment. Charge effects also redshift excitations in the higher-energy optical conductivity.

Vanadate nanoscrolls were prepared by an initial sol–gel reaction followed by hydrothermal treatment, as described previously.^{18,24} Appropriate amines ($\text{C}_n\text{H}_{2n+1}\text{NH}_2$ with $n = 4–18$) were employed as the structure-directing agent. Ion exchange was preformed by stirring a mixture of vanadate nanoscrolls and MCl_2 ($\text{M} = \text{Mn}^{2+}$, Zn^{2+} , and Na^+) for 2 h in ethanol/water mixture. The spectroscopic experiments were carried out over a wide energy range (4 meV to 6.2 eV; $30–50000 \text{ cm}^{-1}$) using a series of spectrometers.¹⁸ Variable temperature work was done between 4.2 and 300 K using an open-flow helium cryostat and temperature controller. The optical constants were calculated by a Kramers–Kronig analysis of the measured reflectance: $\tilde{\epsilon}(\omega) = \tilde{\epsilon}_1(\omega) + i\tilde{\epsilon}_2(\omega) = \tilde{\epsilon}_1(\omega) + (4\pi i/\omega)\tilde{\sigma}_1(\omega)$.²⁷

Figure 2 shows the optical conductivity of the pristine VO_x scrolls and the Mn^{2+} -substituted compounds at room temperature. The pristine scrolls display semiconducting behavior, with clearly resolved vibrational modes below 1000 cm^{-1} and a low background conductivity. These modes were previously assigned as V–O–V axial and equatorial stretching, V–O bending, and screw-like motion of the scrolls.¹⁸ Subtle spectral changes occur when the amine template is exchanged for Mn^{2+} , Zn^{2+} , or Na^+ . In the Mn^{2+} -substituted compound (Figure 2), the optical conductivity develops a broad electronic background in the far-infrared region, with strong phonons riding top of this excitation. The Fano-like lineshapes of several phonons, especially those near 250 and 380 cm^{-1} , indicate that the background is electronic in nature.²⁸ The maximum in the background conductivity near 500 cm^{-1} (green dashed line, Figure 2) indicates that the electronic excitation is pinned. A width of $\sim 400–500 \text{ cm}^{-1}$ is observed. Extrapolating $\sigma_1(\omega)$ to zero frequency, we find $\sigma_1(0) \sim 1 \text{ } \Omega^{-1} \text{ cm}^{-1}$. Such a pinned carrier response is characteristic of a weak or “bad” metal rather than a traditional Drude metal and has been observed in other complex oxides.^{29–32} We obtain similar results at low temperature, suggesting that the vanadium centers in both

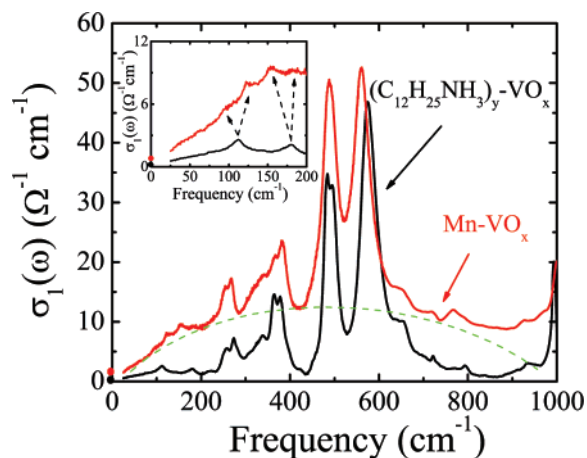


Figure 2. Optical conductivity (300 K) of pristine VO_x scrolls and the Mn^{2+} -exchanged compound in the far-infrared regime. Mode assignments include the following: V–O axial stretching at 945 and 995 cm^{-1} , weak V–O–V equatorial stretching at 790 and 866 cm^{-1} , V–O–V equatorial stretching at 585, 652, and 727 cm^{-1} , V–O–V axial stretching at 486 and 498 cm^{-1} , V–O bending at between 179 and 381 cm^{-1} , and screw-like motion of the scroll at 113 cm^{-1} .¹⁸ The dashed green line guides the eye, highlighting the additional localized carrier contribution in the substituted scrolls. The inset shows a magnified view of the low-frequency response of pristine and Mn^{2+} -exchanged scrolls. The extrapolated dc conductivity is indicated by filled circles at $\omega = 0$ in both panels.

pristine and ion-exchanged scrolls are charge-disproportionated, with V^{4+} and V^{5+} centers rather than the mixed valent state ($\text{V}^{4.5+}$) that might be anticipated for a highly conducting material.

On the basis of the observation of a pinned electronic excitation in the far infrared, the ion-exchange processes does add carriers to the scrolled vanadates. The carriers are not, however, mobile in the ion substituted scrolls. Single-scroll scanning tunneling microscope measurements are in progress to complement this spectroscopic work with local dI/dV measurements. Previous individual tube measurements of Li^+ -exchanged scrolls actually showed a decrease in conductivity with Li^+ hole doping.¹⁹

We now discuss the evolution of the electronic structure of the nanoscrolls due to the metal exchange process within a heuristic correlated-electron model. We use an “effective” band picture, even though a localized description may be more suitable for charge-disproportionated V-oxides,³³ in order to maintain continuity with the existing literature.¹⁹ The pristine scrolls, depicted in Figure 3a, are semiconductors with an optical gap of ~ 0.5 eV.¹⁸ This gap originates from a superposition of both V on-site d-to-d excitations and V^{4+} to V^{5+} charge-transfer excitations.¹⁸ Thus, charge disproportionation already exists in the pristine material. Optical gaps with similar magnitude are observed in bulk VO_2 , ladder-like $\alpha\text{-NaV}_2\text{O}_5$, tubular $\text{Na}_2\text{V}_3\text{O}_8$, and certain molecular magnets.^{34–37} Within the rigid band scenario, the metal-exchange process merely involves charge injection into the V 3d conduction band, which is now partially filled (see Figure 3d).¹⁹ The spectral response of the Mn^{2+} -substituted nanoscrolls in Figure 2, however, clearly precludes the metallic state expected from the bandfilling model. Even if the partially filled band of Figure 3d is split due to chemical

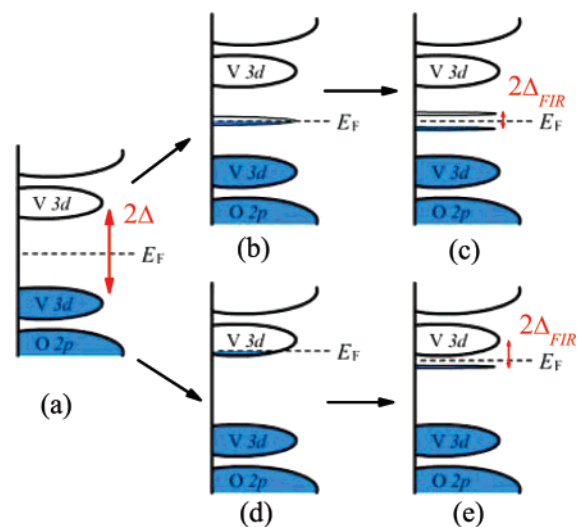


Figure 3. Schematic representation of possible electronic structure changes resulting from the ion-exchange process in the scrolled vanadates. (a) Band structure of pristine vanadium oxide nanoscrolls. Here, 2Δ denotes the ~ 0.5 eV optical gap.¹⁸ (b) Schematic view in which ion exchange adds carriers to a new defect-level band that forms near E_F . (c) Cartoon view in which the new charge defect band splits because of the Madelung energy difference that exists in any charged system, electron–electron interactions, and/or chemical disorder effects. Here, $2\Delta_{\text{FIR}}$ represents the pinned low-energy electronic excitation. This structure will likely have a relatively narrow bandwidth because the excitation is between split defect levels. (d) Alternate approach to the exchange process in which ion exchange adds carriers within the rigid band model.¹⁹ A metallic state might be anticipated to arise from the partially filled band. (e) Schematic view in which the V 3d band splits because of chemical disorder effects. Here, $2\Delta_{\text{FIR}}$ represents a possible low-energy excitation, although it might be anticipated to display a wider bandwidth than that in scheme c because of joint density of states considerations.

disorder effects (Figure 3e), the resulting low-energy excitation would be fairly broad due to joint density of states considerations in which the narrow occupied level below E_F is coupled to the wider empty conduction band arising from the V 3d states.

We believe that the optical response indicates that the ion-exchange process injects charges that are strongly localized due to disorder and Madelung energy considerations. Any charge introduced into the system can, in principle, reduce a V^{5+} to a V^{4+} ion. This extra electron remains pinned, however, as Mn^{2+} ions will “bind” preferentially (though not entirely) to the oxygen atoms bonded to a V^{4+} ion than to a V^{5+} ion because proximity to a V^{5+} ion would raise the Madelung energy substantially. Thus, even in the doped system, there is a barrier to electron hopping between neighboring V^{4+} and V^{5+} ions. Within the effective band model, therefore, the charging process leads to strongly localized deep defect levels as shown in Figure 3b. The dc conductivity may be dominated by hopping between the disordered V^{4+} and V^{5+} ions. The nonbonding character of the localized levels gives them their narrow widths. The local potentials of the two kinds of ions continue to be different due to electron–electron repulsions between neighboring V^{4+} – V^{4+} ions and long-range Madelung energy involving the Mn^{2+} ions. We have depicted this in Figure 3c by an

energy splitting between “occupied” (predominantly V^{4+}) and “unoccupied” (predominantly V^{5+}) defect levels. A dipole-allowed transition between these split defect levels would be consistent with a localized charge excitation rather than a traditional metallic response in the low-energy region of the optical conductivity. Such a feature would be relatively narrow, consistent with the 400–500 cm^{-1} line width observed in the spectrum of Mn^{2+} -substituted scrolls. The above localized picture is in better accord with our experimental results for the pristine and Mn^{2+} -exchanged scrolls.

Careful examination of vibrational mode patterns can also provide information on the ion-exchange process, although in this case we must account for both charge and structural modifications. This analysis is possible because vibrational features are observed in both the pristine and ion-exchanged materials. In the pristine vanadium oxide nanoscrolls, the mode at $\sim 575 \text{ cm}^{-1}$ is assigned as the V–O–V equatorial stretch.¹⁸ This mode is very sensitive to curvature, widening as the size of the amine template is reduced, characteristic of a more strained lattice.¹⁸ The V–O–V equatorial stretching mode (Figure 2) redshifts with ion substitution, moving from $\sim 575 \text{ cm}^{-1}$ in the pristine scrolls, to $\sim 570 \text{ cm}^{-1}$ in Na^+ and $\sim 560 \text{ cm}^{-1}$ in Mn^{2+} -exchanged compounds. Similar shifts in peak position are also observed in other doped and intercalated vanadates.^{38,39} From a structural point of view, the red-shifted V–O–V equatorial stretching mode in the scrolled vanadates is unexpected because X-ray results indicate that the interlayer distance decreases as the smaller metal ions replace the larger amines (from 27.2 to 10.5 Å).^{16,21} The V–O–V equatorial stretching mode might therefore be expected to widen in the substituted scrolls because of their increased curvature, but the center peak position ought to be relatively insensitive to size.¹⁸ Ion exchange also adds charge to the scrolls. We attribute changes in the V–O–V equatorial stretching-mode position (Figure 2) to charging effects that overcome the aforementioned local strain that tends to widen and slightly harden the V–O–V resonance. This overall softening trend ($\sim 575 \text{ cm}^{-1}$ in the pristine scrolls to $\sim 560 \text{ cm}^{-1}$ in the Mn^{2+} -substituted compound) confirms that the ion-exchange process adds carriers to the scrolls. The sharp, unscreened vibrational features in the ion-substituted scrolls, however, show that the carriers are not mobile, consistent with the observation of a pinned charge excitation in the far infrared. The metal-exchange process also leads to some chemical disorder, as evidenced by the splitting of a low-frequency bending motion ($\sim 179 \text{ cm}^{-1}$) and the screw-like mode of the scroll at $\sim 112 \text{ cm}^{-1}$ that is analogous to the radial breathing mode in carbon nanotubes (inset, Figure 2). Disorder in Cu^{2+} -exchanged nanoscrolls has been reported recently as well.²⁵

Figure 4 displays the 300 K optical conductivity of the pristine VO_x scrolls and the Mn^{2+} -exchanged compound over a broader energy range. With the exception of the aforementioned bound carrier excitation localized in the far infrared (Figure 2), the spectrum of the ion-exchanged scrolls is similar to that of the pristine compound, in line with the fact that these high-energy excitations originate from the

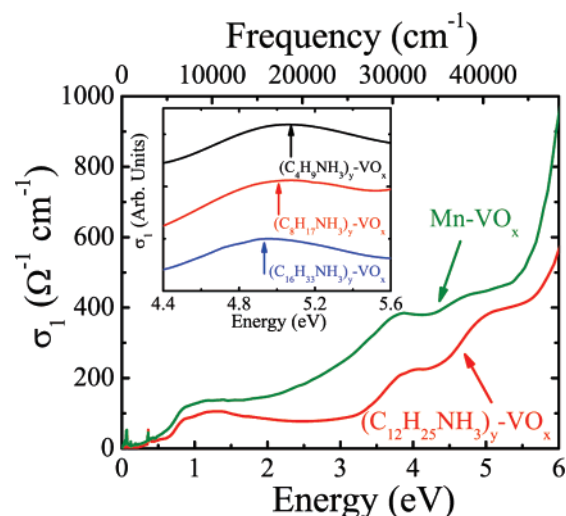


Figure 4. Expanded view of the 300 K optical conductivity of pristine VO_x scrolls and the Mn^{2+} -exchanged compound. The inset shows a close-up view of the $\sim 5 \text{ eV}$ excitation, which changes modestly with sheet distance in the unsubstituted scrolls.¹⁸ In the inset, the curves are offset for clarity.

vanadium oxide framework.^{18,40} Both materials display similar $\sim 0.5 \text{ eV}$ optical gaps and excitations centered near 1 eV that originate from a superposition of V d-to-d on-site excitations and V^{4+} to V^{5+} charge-transfer excitations.¹⁸ The O p to V d charge-transfer excitations at ~ 3.9 and $\sim 5.0 \text{ eV}$ redshift with ion substitution. The fact that this is a charge (rather than size) effect is evident from a comparison of the data in the inset of Figure 4. Here, the excitation centered at $\sim 5.0 \text{ eV}$, which is probably polarized in the radial direction, shifts to higher energy as the size of the amine template decreases (corresponding to a reduction in the interlayer distance).¹⁸ The 3.9 eV feature does not change with curvature.¹⁸ The Mn^{2+} -substituted scrolls display the opposite trend, indicating that charge effects also modify the charge-transfer excitations. First-principles electronic calculations will offer microscopic insight into this problem.

In summary, we measured the optical spectra of pristine and Mn^{2+} -substituted vanadium oxide nanoscrolls in order to understand the charge dynamics in the pristine and metal-exchanged materials and to test the applicability of the rigid band model. In contrast to expectations from the rigid band model, the spectra display a pinned low-energy electronic excitation in the Mn^{2+} -substituted nanoscrolls rather than a traditional metallic response. We propose that the injected charge is localized because of disorder and Madelung energy effects. Our model is consistent with inhomogeneous charge disproportionation (V^{4+} and V^{5+}) in both the pristine and the ion-exchanged materials and explains the observed far-infrared charge localization. Analysis of the vibrational properties shows that the 575 cm^{-1} V–O–V equatorial stretching mode redshifts with ion substitution, indicating that ion exchange modifies both the local curvature and the charge environment. Charge effects also redshift two high-energy electronic excitations.

Acknowledgment. Work at the University of Tennessee is supported by the Materials Science Division, Office of

Basic Energy Sciences at the U.S. Department of Energy under Grant no. DE-FG02-01ER45885. Research at Binghamton is supported by the Division of Materials Research, National Science Foundation under Grant nos. 0313963 and 0705657. Work at the University of Arizona is supported by Materials Science Division, Office of Basic Energy Sciences at the U.S. Department of Energy under Grant no. DE-FG02-06ER46315. We thank H. Zhao for constructing Figure 1b and M. Suzuki for useful discussions.

References

- (1) Rao, C. N. R.; Nath, M. *Dalton Trans.* **2003**, 1, 1.
- (2) Halford, B. *Chem. Eng. News* **2005**, 83, 30.
- (3) Tenne, R. *Nat. Nanotechnol.* **2006**, 1, 103.
- (4) Moses, M. J.; Fetting, J. C.; Wichhorn, B. W. *Science* **2003**, 300, 778.
- (5) Wu, Y.; Messer, B.; Yang, P. *Adv. Mater.* **2001**, 13, 1487.
- (6) Krumeich, F.; Muhr, H.-J.; Niederberger, M.; Bieri, F.; Schnyder, B.; Nesper, R. *J. Am. Chem. Soc.* **1999**, 121, 8324.
- (7) Muhr, H.-J.; Krumeich, F.; Schönholzer, U. P.; Bieri, F.; Niederberger, M.; Gauckler, L. J.; Nesper, R. *Adv. Mater.* **2000**, 12, 231.
- (8) Wörle, M.; Krumeich, F.; Bieri, F.; Muhr, H.-J.; Nesper, R. *Z. Anorg. Allg. Chem.* **2002**, 628, 2778.
- (9) O'Dwyer, C.; Navas, D.; Lavayen, V.; Benavente, E.; Santa Ana, M. A.; González, G.; Newcomb, S. B.; Sotomayor Torres, C. M. *Chem. Mater.* **2006**, 18, 3016.
- (10) Zavalij, P. Y.; Whittingham, M. S. *Acta Crystallogr., B* **1999**, 55, 627.
- (11) Wang, Y.; Cao, G. *Chem. Mater.* **2006**, 18, 2787.
- (12) Marezio, M.; McWhan, D. B.; Dernier, P. D.; Remeika, J. P. *J. Solid State Chem.* **1973**, 6, 213.
- (13) Chakraverty, B. K.; Sienko, M. J.; Bonnerot, J. *Phys. Rev. B* **1978**, 17, 3781.
- (14) Ohama, T.; Isobe, M.; Yasuoka, H.; Ueda, Y. *J. Phys. Soc. Jpn.* **1997**, 66, 545.
- (15) Niederberger, M.; Muhr, H.-J.; Krumeich, F.; Bieri, F.; Günther, D.; Nesper, R. *Chem. Mater.* **2000**, 12, 1995.
- (16) Reinoso, J. M.; Muhr, H.-J.; Krumeich, F.; Bieri, F.; Nesper, R. *Helv. Chim. Acta* **2000**, 83, 1724.
- (17) Wang, X.; Liu, L.; Bontchev, R.; Jacobson, J. *Chem. Commun.* **1998**, 1009.
- (18) (a) Cao, J.; Choi, J.; Musfeldt, J. L.; Lutta, S.; Whittingham, M. S. *Chem. Mater.* **2004**, 16, 731. (b) Cao, J.; Choi, J.; Musfeldt, J. L.; Lutta, S.; Whittingham, M. S. *Nanoscale Materials: From Science to Technology*; Nova Science Publishers: New York, 2006; Chapter 21; p 231.
- (19) Krusin-Elbaum, L.; Newns, D. M.; Zeng, H.; Derycke, V.; Sun, J. Z.; Sandstrom, R. *Nature* **2004**, 431, 672.
- (20) Nordlinder, S.; Nyholm, L.; Gustafsson, T.; Edstrom, K. *Chem. Mater.* **2006**, 18, 495.
- (21) Doble, A.; Ngala, K.; Yang, S.; Zavalij, P. Y.; Whittingham, M. S. *Chem. Mater.* **2001**, 13, 4382.
- (22) Xu, J.-F.; Czerw, R.; Webster, S.; Carroll, D. L.; Ballato, J.; Nesper, R. *Appl. Phys. Lett.* **2002**, 81, 1711.
- (23) Vavilova, E.; Hellmann, I.; Kataev, V.; Täschner, C.; Büchner, B.; Klingeler, R. *Phys. Rev. B* **2006**, 73, 144417.
- (24) Lutta, S.; Doble, A.; Ngala, K.; Yang, S.; Zavalij, P. Y.; Whittingham, M. S. *Mater. Res. Soc. Symp.* **2002**, 703, V8.3.
- (25) Souza Filho, A. G.; Ferreira, O. P.; Santos, E. J. G. P.; Mendes Filho, J.; Alves, O. L. *Nano. Lett.* **2004**, 4, 2099.
- (26) *Graphite Intercalation Compounds and Applications*; Enoki, T., Suzuki, M., Endo, M., Eds.; Academic Press: New York 2003.
- (27) Wooten, F. *Optical Properties of Solids*; Academic Press: New York, 1972; Chapter 6.
- (28) Fano, U. *Phys. Rev.* **1961**, 124, 1886.
- (29) Liu, H. L.; Tanner, D. B.; Berger, H.; Margaritondo, G. *Physica C* **1999**, 311, 197.
- (30) Choi, J.; Musfeldt, J. L.; He, J.; Jin, R.; Thompson, J. R.; Mandrus, D.; Lin, X. N.; Bondarenko, V. A.; Brill, J. W. *Phys. Rev. B* **2004**, 69, 085120.
- (31) Zhu, Z.-T.; Musfeldt, J. L.; Teweldemedhin, Z. S.; Greenblatt, M. *Phys. Rev. B* **2002**, 65, 214519.
- (32) Cao, J.; Haraldsen, J. T.; Rai, R. C.; Brown, S.; Musfeldt, J. L.; Wang, Y. J.; Wei, X.; Apostu, M.; Suryanarayanan, R.; Revcolevschi, A. *Phys. Rev. B* **2006**, 74, 045113.
- (33) Seo, H.; Fukuyama, H. *J. Phys. Soc. Jpn.* **1998**, 67, 2602. Mostovoy, M. V.; Khomskii, D. I. *Solid State Commun.* **2000**, 113, 159.
- (34) Thalmeier, P.; Fulde, P. *Europhys. Lett.* **1998**, 44, 242.
- (35) Verleur, H. W.; Barker, A. S., Jr.; Berglund, C. N. *Phys. Rev.* **1968**, 172, 788.
- (36) Long, V. C.; Zhu, Z.; Musfeldt, J. L.; Wei, X.; Koo, H.-J.; Whangbo, M.-H.; Jegoudez, J.; Revcolevschi, A. *Phys. Rev. B* **1999**, 60, 15721.
- (37) Choi, J.; Musfeldt, J. L.; Wang, Y. J.; Koo, H.-J.; Whangbo, M.-H.; Galy, J.; Millet, P. *Chem. Mater.* **2002**, 14, 924.
- (38) Barbour, A.; Luttrell, R. D.; Choi, J.; Musfeldt, J. L.; Zipse, D.; Dalal, N. S.; Boukhvalov, D. W.; Dobrovitski, V. V.; Katsnelson, M. I.; Lichtenstein, A. I.; Harmon, B. N.; Kögerler, P. *Phys. Rev. B* **2006**, 74, 014411.
- (39) Cazzanelli, E.; Mariotto, G.; Passerini, S.; Decker, F. *Solid State Ionics* **1994**, 70–71, 412.
- (40) Choi, J.; Musfeldt, J. L.; Rudko, G. Yu.; Jegoudez, J.; Revcolevschi, A. *Solid State Commun.* **2002**, 123, 167.
- (41) Mn^{2+} itself does not contribute strongly to the optical response because it is structurally well-isolated and not coordinated to other nearby centers.

NL071002L